Ag surface plasmon enhanced double-layer antireflection coatings for GaAs solar cells

Wang Yanshuo(王彦硕)[1,†], Chen Nuofu(陈诺夫)[1,2], Zhang Xingwang(张兴旺)[1], Yang Xiaoli(杨晓丽)[1], Bai Yiming(白一鸣)[1], Cui Min(崔敏)[1], Wang Yu(汪宇)[1], Chen Xiaofeng(陈晓锋)[1], and Huang Tianmao(黄添懋)[1]

(1 Key Laboratory of Semiconductor Materials Science, Institute of Semiconductors, Chinese Academy of Sciences, Beijing 100083, China)

(2 National Laboratory of Micro-Gravity, Institute of Mechanics, Chinese Academy of Sciences, Beijing 100080, China)

Abstract: Surface plasmon enhanced antireflection coatings for GaAs solar cells have been designed theoretically. The reflectance of double-layer antireflection coatings (ARCs) with different suspensions of Ag particles is calculated as a function of the wavelength according to the optical interference matrix and the Mie theory. The mean dielectric concept was adopted in the simulations. A significant reduction of reflectance in the spectral region from 300 to 400 nm was found to be beneficial for the design of ARCs. A new SiO_2/Ag–ZnS double-layer coating with better antireflection ability can be achieved if the particle volume fraction in ZnS is 1%–2%.

Key words: antireflection coating; surface plasmon resonance; GaAs solar cells
DOI: 10.1088/1674-4926/30/7/072005 **PACC:** 4280X; 7865K; 7145

1. Introduction

The performance of antireflection coatings (ARCs) will greatly affect the efficiency of solar cells[1]. Therefore, high-quality ARCs have become one of the vital features of high-efficiency solar cells. In recent decades, many meaningful achievements have been made in both theoretical and experimental studies. Bouhafs *et al.*[2] designed Ta_2O_5, ZnS, and Al_2O_3 single-layer antireflection coatings (SLARCs), MgF_2/ZnS double-layer antireflection coating (DLARC), and MgF_2/Al_2O_3/ZnS triple layer ARC systems, in which the reflectance was calculated by using transfer matrixes and the reflectance of the ARC systems on a silicon substrate was measured. Additionally, Lee *et al.*[3] designed a MgF_2/CeO DLARC. Bai *et al.*[4] modified the thickness of DLARC layers considering the weighted mean reflection and the dispersion effect of the coating materials. However, most of the designs mentioned above focused on the visible (390–760 nm) part of the sun's spectrum. In the ultraviolet (UV) and the infrared (IR) sections, especially in the UV area, reflectance increases distinctly to 40%[2–4]. For photovoltaic solar cells, high reflectance in the UV region will waste energy.

In recent years, surface plasmons, which are collective oscillations of the electrons in conductors, have been extensively researched for biologic and luminescence applications[5]. However, on the whole, there has not been extensive study of photovoltaic applications of surface plasmons. Very recently, Catchpole and Pillai[6,7] investigated the suitability of localized surface plasmons on silver nanoparticles for enhancing the absorbance of silicon solar cells in the IR region. They modeled Ag particles as scattering luminescent emitters and made use of the broadened emission peak to facilitate the near band (in IR region) light absorption in a Si thin film. Being different from thin film silicon solar cells, the absorbance of III-V thin film solar cells or bulk silicon solar cells is sufficient, but the high reflectance of ARCs in the UV region limits the absorption of these cells. In this paper, we focus on reducing the ARC reflection in the UV region. For this purpose, surface plasmons resonance enhanced ARCs are theoretically designed. On metal nanoparticles, the oscillation leads to a strong extinction of incident light at a certain particular frequency, which is termed the surface plasmon resonance (SPR) frequency[5]. The surface plasmon resonance frequency depends most strongly on the material that forms the nanoparticle, but can be tuned by varying the shape of the nanoparticle and surrounding dielectric environment. We pin our hopes on making use of these extinction properties by planting metal particles into ARC layers to reduce the reflections, which is a combination of DLARC and SPR enhanced scattering. Based on the standard optical theorem and Mie's light scattering theory[8], models of the new ARC system are simulated. The simulation results and further use of SPR in solar cells are discussed in later sections.

2. Calculation method and modeling

Our simulation framework has been made for calculating the reflectance of designed ARCs in this section. The standard optical theory and the basic surface plasmon resonance theory are introduced first, followed by the model structures and the simulation parameters.

† Corresponding author. Email: yswang@semi.ac.cn
Received 21 October 2008, revised manuscript received 8 January 2009

2.1. Matrix method

The matrix method[9] is frequently used to calculate the reflection from a multilayer system. The system reflection R is calculated by

$$R = \left|\frac{n_0 - Y}{n_0 + Y}\right|^2, \tag{1}$$

where Y is termed the optical admittance, which is a function of the thickness and the refractive index of each layer, and $n_0 = 1$ at the interface to the air. More detailed descriptions can be found in Refs. [4, 9].

Hence, the system reflection at a certain wavelength can be calculated once all the thicknesses and refractive indices of each layer are determined. Since the refractive index of the layer medium can be obtained from the existing literature, we just need to determine the refractive index of the composite layer.

2.2. Optical extinction of metal spheres (Mie theory)

The optical extinction on metal particles was interpreted by Mie[8] in 1908 by solving Maxwell's equations. Both particle absorption and (Rayleigh) scattering contribute to extinction, i.e., $C_{\text{ext}} = C_{\text{sca}} + C_{\text{abs}}$. An approximate expansion is given by Bohren and Huffman[10].

$$C_{\text{sca}} = \frac{8\pi}{3} k_{\text{vac}}^4 R^6 \left|\frac{\tilde{m}^2 - 1}{\tilde{m}^2 + 2}\right|^2, \quad C_{\text{abs}} \cong 4\pi k_{\text{vac}} R^3 \text{Im}\left[\frac{\tilde{m}^2 - 1}{\tilde{m}^2 + 2}\right]. \tag{2}$$

Here, R is the radius of the spheres causing the extinction, which have been expanded in terms of $x = \frac{2\pi}{\lambda} nR$, where $\tilde{n}$ is the complex refractive index of the medium $\tilde{n} = n + \text{i}k$ and $\tilde{m}^2 = \frac{\tilde{\varepsilon}_{\text{sph}}}{\tilde{\varepsilon}_{\text{m}}}$ is the ratio of the complex dielectric function of the spheres to the complex dielectric function of the medium.

To describe the optical properties of a composite with suspended metal particles, an effective dielectric function theory was presented by Maxwell–Garnet[11, 12], in which the effective dielectric function of the composite is given by

$$\tilde{\varepsilon} = \tilde{\varepsilon}_{\text{m}} \frac{1 + 2f(\tilde{\varepsilon}_{\text{sph}} - \tilde{\varepsilon}_{\text{m}})/(\tilde{\varepsilon}_{\text{sph}} + 2\tilde{\varepsilon}_{\text{m}})}{1 - f(\tilde{\varepsilon}_{\text{sph}} - \tilde{\varepsilon}_{\text{m}})/(\tilde{\varepsilon}_{\text{sph}} + 2\tilde{\varepsilon}_{\text{m}})}, \tag{3}$$

where f is the volume fraction of metal particles in the composite. The complex refractive index $\tilde{n}$ of the effective composite layer can be extracted from the relation $\tilde{\varepsilon} = \tilde{n}^2 = (n + \text{i}k)^2$. Thus, one can plug these complex refractive indices into the optical matrix (mentioned in Section 2.1) of the composite layer and deduce the reflection of the multilayer system.

If the suspension of metal particles is extremely dilute ($f < 1\%$), each particle contributes approximately linearly to the total extinction for the material and the refractive index n is unchanged[10]. The effective extinction coefficient through the composite material is given by[13]

$$k = k_{\text{m}} + \frac{3}{2} f n \text{Im}\left(\frac{n^2}{\tilde{n}^2} \frac{\tilde{m}^2 - 1}{\tilde{m}^2 + 2}\right). \tag{4}$$

Generally speaking, the noble metals Au, Ag, and Cu have distinctly sharper resonances than non-noble metals, such as Cr, Fe, Ni, As, and Er[5, 14]. In particular, Ag has the most suitable resonance frequency in the UV region[15, 16].

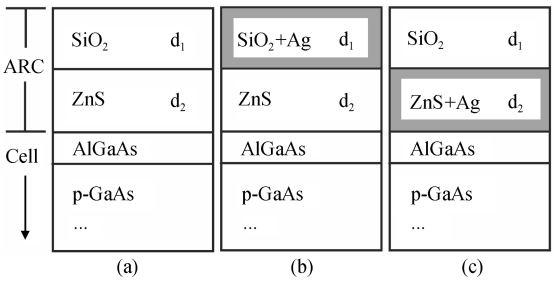

Fig. 1. Structures of ARCs: (a) Common structure of SiO_2/ZnS double-layer antireflection coating; (b), (c) Modified structures of ARC.

2.3. Modeling

As mentioned above, we target at an enhancement close to the UV region, where antireflection in a traditional SiO_2/ZnS coatings is weak. We will investigate the effect of scattering by Ag metal nanoparticles in SiO_2 or ZnS layers, and compare the antireflection enhancement for GaAs cells.

The new designed ARC structures are shown in Figs. 1(b) and 1(c). These are modified forms of normal DLARC (see Fig. 1(a)). Ag particles are suspended in the selected layer. For simple simulations, we suppose that the particle distributions are uniform in the composite layers.

As ARC is a kind of multilayer system, the reflectance of the structures (b) and (c) can be calculated from Eq. (1) when the optical properties of composite layers are derived from Eqs. (3) and (4).

2.4. Parameters for simulations

The complex refractive indices of SiO_2, ZnS, Ag, AlGaAs and so on are taken from Palik's work[17] and Wemple's work[18, 19]. The particle diameter is designed larger than 80 nm. The volume fraction of particles ranges from 1% to 10%. Each layer thickness is determined by[20]

$$\bar{n}_{\text{j}} d_{\text{j}} = \frac{\text{j}\lambda}{4}. \tag{5}$$

where $\bar{n}_{\text{j}}$ is the weighted average refractive index given by Ref. [4].

3. Results and discussions

3.1. Reflections of systems with extreme dilute suspension

The reflection calculated from Eqs. (1) and (4) is shown in Fig. 2(a) for a 1% volume fraction of metal spheres in SiO_2 and in ZnS media.

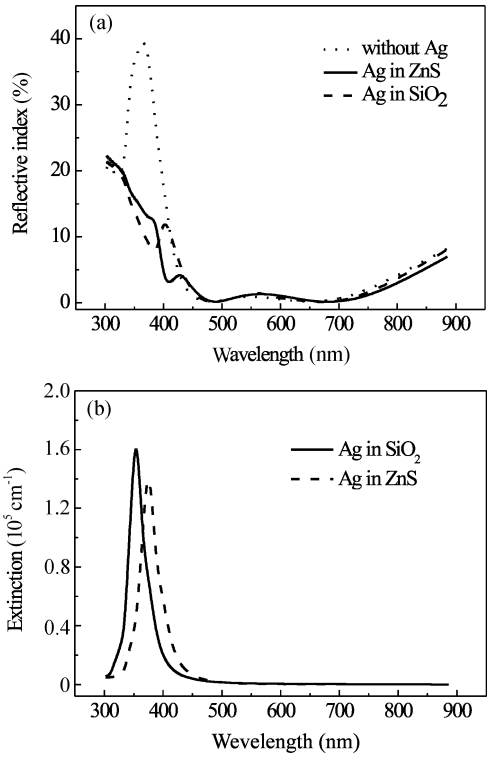

Fig. 2. (a) Reflectance of double-layer antireflection coatings as a function of wavelength; (b) Extinction of an Ag–SiO_2 and an Ag–ZnS composite as a function of wavelength.

Since the volume fraction of metal spheres is small, the reflection changes in the visible region are negligible. Near the resonance frequency, the extinction contribution becomes comparable to the reflection, and the reflectance correspondingly becomes lower. Particles in SiO_2 provide a resonance wavelength near 370 nm. Similarly, a ZnS medium tunes the wavelength as high as 400 nm. It is in good agreement with their different resonance frequencies (see Fig. 2(b)), which were calculated from Eq. (2). And particles in a ZnS layer have a larger extinction contribution in Fig. 2(a) than in a SiO_2 layer, because of the greater thickness.

It should be pointed out that the layer thicknesses d_1 in Fig. 1(b) and d_2 in Fig. 1(c) are 94.2 and 119.5 nm. Therefore, the diameter of Ag particles should be less than 94 or 119 nm. In other words, the solid particles are arranged in a plan with our previous settings of $D > 80$ nm.

3.2. Reflections of systems with a dilute suspension

As an Ag–ZnS composite shows a better light trapping ability in the spectral region needed, we will mainly focus on the influence of the particle volume fraction of the ZnS layer in this section. The corresponding reflections of the modified ARC systems were calculated from Eqs. (1) and (3) by changing the particle volume fraction from 2% to 10%. Partial calculated data are shown in Fig. 3.

The plot shows that the enhancement of the antireflection at the resonance wavelength is significant for a larger volume fraction compared with Fig. 2, and there tends to be a reduction in the antireflection towards larger particle sizes at other

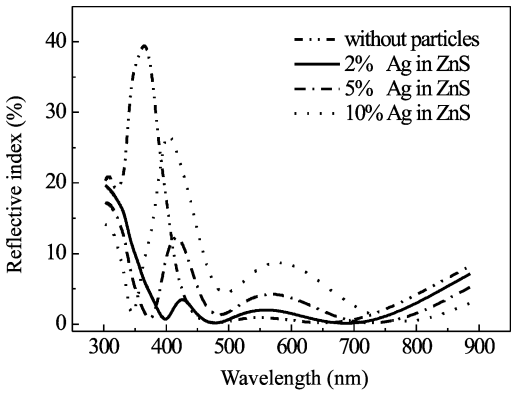

Fig. 3. Reflectance of DLARCs as a function of wavelength. The curves correspond to particle volume fractions of 2%, 5%, and 10%.

wavelengths. Nevertheless, at all wavelengths there is an expansion of the antireflection region. However, for the model we designed, the expansion of the AR region is not very prominent, whereas the reduction in the antireflection is quite significant. The reason for this is that the metal particles with larger volume fraction will affect not only the extinction part of the complex refractive index, but also the refractive part. This causes a distinct refractive dispersion effect. As a weighted average layer thickness is used in the simulations, the dispersion effect of the refractive index, therefore, leads to a dispersion of the reflectance. It is easy to understand the influence of the higher volume fraction in the limited case. If $f = 100\%$, the composite layer becomes metallic and the reflection will be apparently enhanced. In sum, ARCs show a better antireflection capability when the particle volume fraction is $f = 1\%$–2%.

3.3. Contribution of scattering

From what was calculated above, it is seen that there is a considerable enhancement of the antireflection caused by the extinction characteristics of metal particles. However, only the scattering section is helpful to the solar cell, as we mentioned before. As seen from Eq. (2), the efficiency of the absorption, scaling with R^3, dominates over the scattering efficiency, which scales with R^6. Obviously, as the particle size increases, the extinction tends to be dominated by scattering, and the scattering efficiency is considered to be an important factor in light trapping.

The contribution of scattering to extinction in Eq. (2) is shown in Fig. 4 for a volume fraction of $f = 1\%$ and for metal spheres with increasing radii from 40 to 46 nm (60 nm). The absorption from the particles contributes largely to the total extinction at a wavelength near 300 nm. The Rayleigh contribution rapidly becomes comparable to the particulate absorption as the wavelength increases. For an extinction at a wavelength larger than 330 nm, scattering will play an important role. The plot also shows that the absorption contributes less to the extinction when the particle diameter increases. With increasing particle diameters, higher terms in the Mie scattering formula Eq. (2) become significant, and Mie resonances will dominate

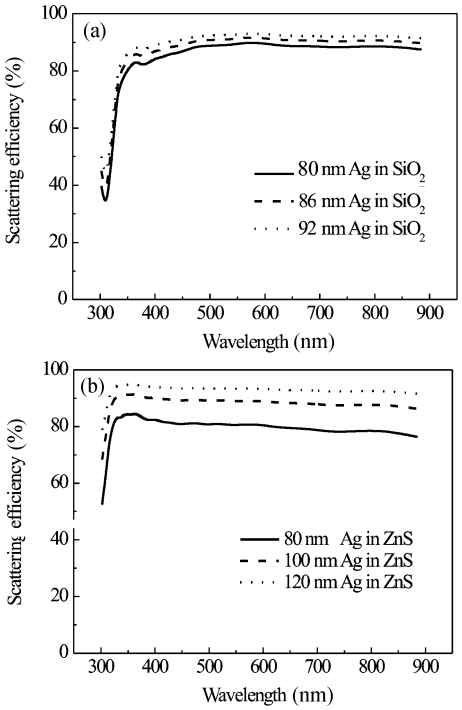

Fig. 4. Absorption efficiency for Ag particles in different media. The curves are for increasing particle diameter at a constant volume fraction $f = 1\%$.

the extinction. We can see that the absorption contribution becomes negligible when the particle diameter increases to 120 nm in a ZnS medium.

For a volume fraction of $f = 2\%$, the scattering efficiency calculated is similar to the result above. In brief, it means that the improvement of the antireflection shown in Fig. 2 and Fig. 3 is mainly due to Rayleigh scattering.

3.4. Extinction in different media

In our photovoltaic research programs, such as tandem solar cells and integrated micro solar cells, ultra-thin GaAs solar cells were frequently designed and made according to our high-integration-density requirements. However, the efficiencies of such cells are limited because of the relatively poor light absorption. For instance, micro solar cells for MEMS are usually designed in an ultra-thin (400 nm) style. The light absorption in these cells is not sufficient near the bandgap (see Fig. 5). As we mentioned in Section 1, the surface plasmon resonance frequency can be tuned by varying the surrounding dielectric environment. Imbedding a metal sphere in a high-dielectric-constant medium will increase the resonance wavelength (red-shift effect), which was correspondingly reflected in Eq. (2) and Fig. 2(b). In addition, the absorbing medium will broaden the range of the resonance extinction[5]. The red-shift effect and the expansion of the resonance provide a probability for the enhancement of light trapping in the high-wavelength region[6].

The composite extinction cross section from Eq. (2) is shown in Fig. 6 for a 1% volume fraction of 80 nm metal spheres in a TiO_2 and in an AlGaAs medium. It should be

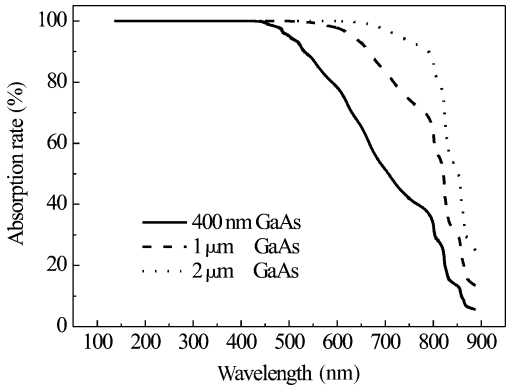

Fig. 5. Absorption rate of different thicknesses of a GaAs layer. The interface reflection is neglected.

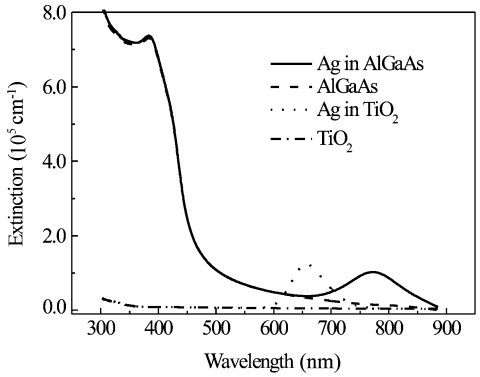

Fig. 6. Composite extinction in an Ag–AlGaAs and an Ag–TiO_2 medium. A high-dielectric-constant medium causes an increasing of the resonance wavelength.

noted that, for AlGaAs, which is an absorbing medium, Equation (2) becomes semi-quantitatively correct, and the free electron model (FEM) for a metal is used here to derive the effective dielectric of the spheres[14]. And the larger absorption in the medium contributes a larger imaginary component to the complex dielectric function of the composite, which broadens the resonance. In particular, in an AlGaAs medium, the resonance is significantly broadened.

If we embed metal particles in a high-dielectric-constant ARC medium such as TiO_2, or in a window medium of the cells, such as AlGaAs, the utilization rate of the incident photons in ultra-thin GaAs solar cells will likely be increased. The red-shift and the broadening effects also potentially promise an alternative method to improve single-layer antireflection coatings.

4. Conclusions

The performance of the modified ARC system is simulated by calculating the system reflection from the standard optical theorem and the Mie theory with different structural parameters, including the complex refractive indices of the medium and the volume fraction of the metal particles. When the particle volume fraction in a ZnS medium is 1%–2%, and the diameter of particles is larger than 100 nm, the calculated enhancement of the antireflection is significant in the near-UV

region for GaAs solar cells. The nanoparticles also have the potential to increase the near band absorption for extra-thin GaAs cells. The simulation contributes to the design and the fabrication of high-quality antireflection coatings of GaAs solar cells.

References

[1] Green M A. Solar cells. New Jersey: Prentice-Hall Inc, 1982

[2] Bouhafs D, Moussi A, Chikouche A, et al. Design and simulation of antireflection coating systems for optoelectronic devices: application to silicon solar cells. Solar Energy Materials and Solar Cells, 1998, 52: 79

[3] Lee S E, Chio S W, Yi J. Double-layer antireflection coating using MgF_2 and CeO_2 films on a crystalline silicon substrate. Thin Solid Films, 2000, 376: 208

[4] Bai Yiming, Chen Nuofu, Dai Ruixuan, et al. Dispersion effect on double-layer anti-reflection coatings of GaAs solar cells. Chinese Journal of Semiconductors, 2006, 27(4): 725 (in Chinese)

[5] Maier S A. Plasmonics: fundamentals and applications. 1st ed. Springer, 2007

[6] Catchpole K R, Pillai S. Surface plasmons for enhanced thin-film silicon solar cells and light emitting diodes. Journal of Luminescence, 2006, 121(2): 315

[7] Pillai S, Catchpole K R, Trupke T, et al. Surface plasmon enhanced silicon solar cells. J Appl Phys, 2007, 101: 093105

[8] Mie G. Beitrage zur optik truber medien, speziell kolloidaler metallosungen. Annalen der Physik, Series IV, 1908, 25(3): 377

[9] Born M,Wolf E. Principles of optics. 5th ed. New York: Pergamon, 1975

[10] Bohren C F, Huffman D. Absorption and scattering of light by small particles. New York: John Wiley, 1983

[11] Cohen R W, Cody G D, Coutts M D, et al. Optical properties of granular silver and gold films. Phys Rev B, 1973, 8: 3689

[12] Toudert J, Babonneau D, Simonot L, et al. Quantitative modeling of the surface plasmon resonances of metal nanoclusters sandwiched between dielectric layers: the influence of nanocluster size shape and organization. Nanotechnology, 2008, 19: 125709

[13] Vollmer M, Kreibig U. Collective excitations in large metal clusters. Springer Berlin, Nuclear Physics Concepts in the Study of Atomic Cluster Physics, 1992, Volume 404

[14] Nolte D D. Optical scattering and absorption by metal nanoclusters in GaAs. J Appl Phys, 1994, 76(6): 3740

[15] Martinez-Castanon G. Martínez J R, Zarzosa G O. Optical absorption of Ag particles dispersed in a SiO_2 amorphous matrix. Journal of Sol-Gel Science and Technology, 2005, 36(2): 137

[16] Kreibig U, Vollmer M. Optical properties of metal clusters. In: Springer Series in Materials. Vol. 25. Science, 1995

[17] Palik E D. Handbook of optical constants of solids. 1st ed. Academic Press, 1997

[18] Wemple S H. Optical dispersion and the structure of solids. Phys Rev Lett, 1969, 23(20): 1156

[19] Wemple S H. Behavior of the electronic dielectric constant in covalent and ionic materials. Phys Rev B, 1971, 3(4): 1338

[20] Flory F R. Thin films for optical systems. 1 st ed. CRC, 1995